

## X-RAY PHOTOELECTRON AND BROADBAND IMPEDANCE SPECTROSCOPY OF $\text{Li}_{1+4x}\text{Ti}_{2-x}(\text{PO}_4)_3$ SOLID ELECTROLYTE CERAMICS

A.F. Orliukas<sup>a</sup>, V. Venckutė<sup>a</sup>, J. Miškinis<sup>b</sup>, V. Kazlauskienė<sup>b</sup>, D. Petrulionis<sup>a</sup>, T. Šalkus<sup>a</sup>,

A. Dindune<sup>c</sup>, Z. Kanepe<sup>c</sup>, J. Ronis<sup>c</sup>, T. Žukauskas<sup>a</sup>, A. Maneikis<sup>d</sup>, and A. Kežionis<sup>a</sup>

<sup>a</sup> Faculty of Physics, Vilnius University, Saulėtekio 9/3, LT-10222 Vilnius, Lithuania

E-mail: vilma.venckute@ff.vu.lt

<sup>b</sup> Institute of Applied Research, Vilnius University, Saulėtekio 9/3, LT-10222 Vilnius, Lithuania

<sup>c</sup> Institute of Inorganic Chemistry, Riga Technical University, Miera iela 34, 2169 Salaspils, Latvia

<sup>d</sup> Semiconductor Physics Institute, Center for Physical Sciences and Technology, A. Goštauto 11, LT-01108 Vilnius, Lithuania

Received 2 July 2013; revised 30 September 2013; accepted 4 December 2013

$\text{Li}_{1+4x}\text{Ti}_{2-x}(\text{PO}_4)_3$  (where  $x = 0.2, 0.5$ ) compounds were synthesized by solid state reaction, and ceramics were sintered. The structure of compounds was studied by X-ray diffraction. Elemental compositions and binding energies of Ti 2p, P 2p, O 1s, and Li 1s core level at the surfaces of  $\text{Li}_{1+4x}\text{Ti}_{2-x}(\text{PO}_4)_3$  ceramics were determined by energy dispersive X-ray spectrometer (EDX) and X-ray photoelectron spectroscopy (XPS). Impedance spectroscopy of the ceramics was performed in the frequency range of 10 Hz–1 MHz by the four-electrode method and in the frequency range of 1 MHz – 3 GHz by the microwave impedance spectrometer. The measurements of electrical properties of the ceramics were carried out in the temperature interval of (300–700) K. The increase of the stoichiometric factor  $x$  of the compounds leads to the increase of bulk conductivities and values of dielectric permittivity.

**Keywords:** XRD, SEM/EDX, XPS, ceramics, impedance spectroscopy, electric conductivity

**PACS:** 66.30.Dn, 79.60.-I, 81.05.Je, 84.32.Ff

### 1. Introduction

A wide variety of  $\text{Li}^+$  ion conducting compounds have been synthesized in the NASICON-type materials and are technologically important for applications as solid electrolytes for batteries and gas sensors [1–4]. The rhombohedral structured (space group  $R\bar{3}c$ )  $\text{LiTi}_2(\text{PO}_4)_3$  compound is a solid electrolyte with fast Li ion transport [3–5]. At room temperature the values of bulk and total conductivities were found to be  $1 \cdot 10^{-2}$  S/m and  $2 \cdot 10^{-4}$  S/m, respectively [3]. The bulk conductivity increase is a result from increase of  $\text{Li}^+$  content in these compounds [4]. It makes them attractive materials for

investigations of the dynamic properties associated with peculiarities of ionic migration. According to [5, 6], in some NASICON-type compounds  $\text{Li}^+$  ions occupy two different energy sites in the lattice what is typical of most NASICON conductors, but the results of nuclear magnetic resonance investigation have shown only one lithium site in the lattice [7]. High ionic conductivity of the above-mentioned NASICON-type structure solid electrolyte compounds stimulate further investigation of their electrical properties in the broadband frequency and temperature ranges and relationship between compositions and transport properties of the materials. For investigations,  $\text{Li}_{1+4x}\text{Ti}_{2-x}(\text{PO}_4)_3$  (where

$x = 0.2, 0.5$ ) powders and ceramics were prepared. The results of the X-ray diffraction (XRD) study, scanning electron microscope with an attached energy dispersive X-ray spectrometer (SEM/EDX), X-ray photoelectron spectroscopy (XPS) of the surface of ceramics, and the results of investigation of the electrical properties of ceramics by impedance spectroscopy are presented.

## 2. Experiment

The stoichiometric mixture of  $\text{Li}_2\text{CO}_3$  (purity 99.999%), extra pure  $\text{NH}_4\text{H}_2\text{PO}_4$ , and  $\text{TiO}_2$  for the powder of  $\text{Li}_{1+4x}\text{Ti}_{2-x}(\text{PO}_4)_3$  (where  $x = 0.2, 0.5$ ) synthesis was used. The powder was synthesized by solid state reaction. The mixture with stoichiometric amounts was placed into ethyl alcohol and milled for 8 hours in an agate mill. After milling, the mixture was heated for 20 h at the temperature  $T = 723$  K. After heating, the mixture was placed into ethyl alcohol and this liquid was milled for 8 h in the planetary mill again. After this process the powder was heated for 8 h at  $T = 1173$  K. The fine powder was dried at  $T = 393$  K for 24 h. The structure parameters were obtained using the *Brucker* D8 Advance equipment at room temperature from the X-ray powder diffraction patterns in the region  $2\theta = 6\text{--}80$  degree, step 0.02 degree, time per step 1–8 sec,  $\text{CuK}_{\alpha 1}$  radiation (40 kV, 40 mA). The lattice parameters were deduced by fitting the XRD patterns with software TOPAS v.4.1 and SCANIX v.2.16 (*Matpol*) [8]. SEM/EDX (TM3000, *Hitachi*) for analysis of chemical composition of investigated compounds was used. For investigation of SEM/EDX, XPS, and electrical properties the ceramic samples were sintered. The powder was uniaxially cold-pressed at 300 MPa. The sintering of  $\text{Li}_{1+4x}\text{Ti}_{2-x}(\text{PO}_4)_3$  ceramic samples with stoichiometric parameters  $x = 0.2, 0.5$  were conducted in air at the temperature  $T = 1363$  and  $923$  K, respectively. The sintering duration of ceramics was 1 h. The binding energies of the constituent elements of the surfaces of ceramics were examined by X-ray photoelectron spectroscopy as in [9] but the XPS was obtained by using  $\text{Al K}_{\alpha}$  ( $h\nu = 1486.6$  eV) radiation at an average of 30 scans with the step size of 0.05 eV. For the measurements of complex conductivity ( $\tilde{\sigma} = \sigma' + i\sigma''$ ), complex specific electrical resistivity ( $\tilde{\rho} = \rho' - i\rho''$ ), and complex dielectric permittivity ( $\tilde{\epsilon} = \epsilon' - i\epsilon''$ ) Pt electrodes were pre-

pared. Pt paste from company *GWENT* was used. For measurements of electrical impedance in the frequency range of  $(10\text{--}1 \cdot 10^5)$  Hz the four-probe method (as in [10]) was used. The measurements in the frequency range of  $(3 \cdot 10^5\text{--}3 \cdot 10^9)$  Hz were performed by the *Agilent* Network Analyzer E5062A connected to the coaxial line, part of the inner conductor of which was replaced by the sample. The impedance of the sample was calculated from the scattering parameters' matrix of the two-port network as in [11].

## 3. Results and discussion

The amounts of up to 0.8 wt. % and 5 wt. % of  $\text{LiTiPO}_5$  and  $\text{Li}_4(\text{P}_2\text{O}_7)$  in compounds with  $x = 0.2$  and  $0.5$ , respectively, were found. The amounts of impurities were estimated from intensities and their square analysis of XRD patterns.  $\text{LiTiPO}_5$  and  $\text{Li}_4(\text{P}_2\text{O}_7)$  belong to the orthorhombic and triclinic symmetry group and are marked with asterisks on the XRD patterns in Fig. 1. At room temperature the  $\text{Li}_{1+4x}\text{Ti}_{2-x}(\text{PO}_4)_3$  (where  $x = 0.2, 0.5$ ) compounds belong to the rhombohedral symmetry (space group  $R\bar{3}c$ ) with six formula units in the unit cell. In Table 1 the lattice  $a$ ,  $c$  parameters, volume  $V$ , theoretical  $d_t$  and relative  $d_r$  densities of the ceramics are presented.

An increase of Li content leads to an increase of the volume of the lattice and decrease of the theoretical density of the compounds. This variation can be caused by the different values of the ionic radii of  $\text{Li}^+$  and  $\text{Ti}^{4+}$  ions. The ionic radii of  $\text{Li}^+$  and  $\text{Ti}^{4+}$  are 0.92 and 0.74 Å, respectively [12]. On the other hand, the analysis of XRD patterns shows the impurities of  $\text{LiTiPO}_5$  and  $\text{Li}_4(\text{P}_2\text{O}_7)$ , which can influence the above-mentioned parameters too. The SEM image of the surface of  $\text{Li}_{1.8}\text{Ti}_{1.8}(\text{PO}_4)_3$  ceramics is presented in Fig. 2. The microstructure of both investigated ceramics is similar and their grain sizes vary in the range from 4 to 10  $\mu\text{m}$ . Figure 3 shows EDX spectra for the grains of ceramics. The results of the investigation of elemental compositions showed a small amount of Al (0.585–0.457 wt. %, the error of this amount is found to be  $\eta \pm 0.035\text{--}0.033$  wt. %) and Si (0.220–0.201 wt. %,  $\eta \pm 0.32\text{--}0.031$  wt. %) impurities in the grains of the investigated ceramics (see the insertions of Fig. 3). These impurities could be from substrates which were used for the sintering of ceramics.

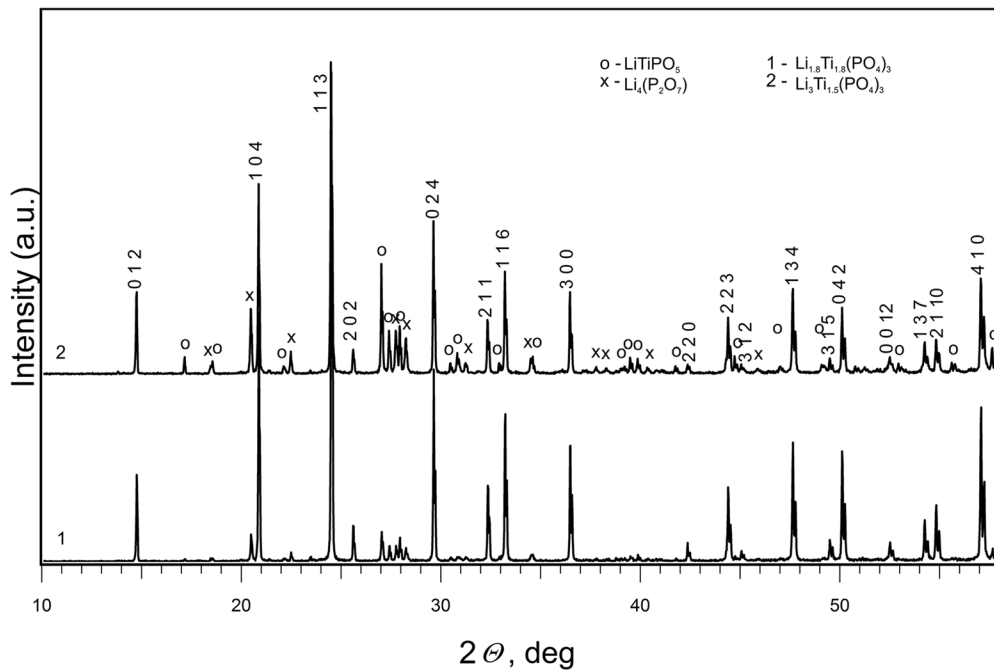


Fig. 1. XRD patterns of  $\text{Li}_{1+4x}\text{Ti}_{2-x}(\text{PO}_4)_3$  (where  $x = 0.2, 0.5$ ) at room temperature.

Table 1. Summary of X-ray diffraction results for  $\text{Li}_{1+4x}\text{Ti}_{2-x}(\text{PO}_4)_3$  (where  $x = 0.2, 0.5$ ) compounds at room temperature.

Compound	Space group	Lattice parameters			Formula units (Z)	Theoretical density $d_p$ , g/cm <sup>3</sup>	Relative density $d_r$ , %
		$a$ , Å	$c$ , Å	$V$ , Å <sup>3</sup>			
$\text{Li}_{1.8}\text{Ti}_{1.8}(\text{PO}_4)_3$	$R\bar{3}c$	8.5162(4)	20.8482(30)	1309.50	6	2.90	95
$\text{Li}_3\text{Ti}_{1.5}(\text{PO}_4)_3$	$R\bar{3}c$	8.5144(5)	20.8762(60)	1310.80	6	2.85	81

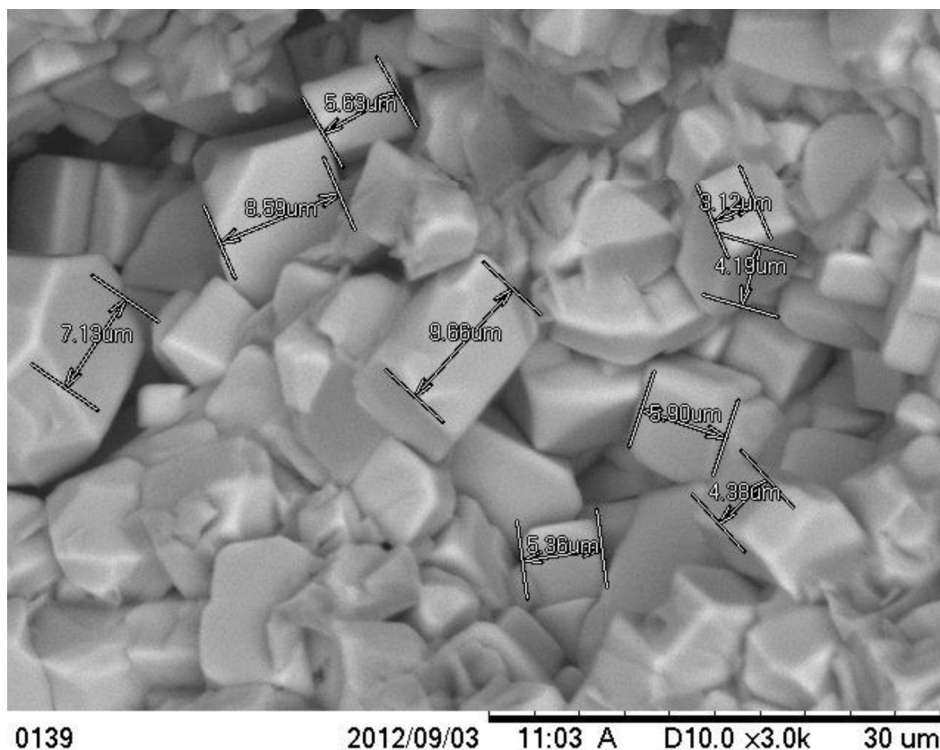


Fig. 2. SEM image of  $\text{Li}_{1.8}\text{Ti}_{1.8}(\text{PO}_4)_3$  ceramics surface.

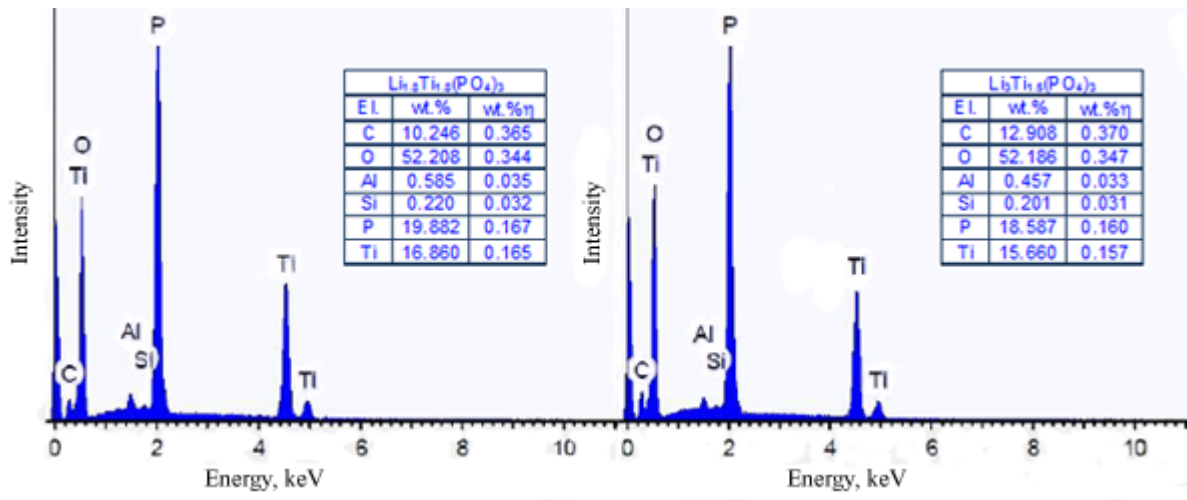


Fig. 3. EDX spectra of the grains of  $\text{Li}_{1+4x}\text{Ti}_{2-x}(\text{PO}_4)_3$  (where  $x = 0.2, 0.5$ ) ceramics surfaces.

To exclude any effects on the values of binding energies due to the charging of the sample during XPS analysis, all data were corrected by a linear shift such that the peak maximum of the C 1s binding energy of adventitious carbon corresponded to 284.6 eV. Ti 2p, P 2p, and O 1s core level XP spectra

of  $\text{Li}_{1+4x}\text{Ti}_{2-x}(\text{PO}_4)_3$  (where  $x = 0.2, 0.5$ ) were fitted. Characteristic Ti 2p, P 2p, O 1s, and Li 1s core level XP spectra of  $\text{Li}_{1+4x}\text{Ti}_{2-x}(\text{PO}_4)_3$  (with  $x = 0.2, 0.5$ ) ceramics are shown in Fig. 4(a–d). The Ti 2p XP spectrum is shown in Fig. 4(a). The spectrum shows a double spin-orbit doublet of Ti 2p spectra as in

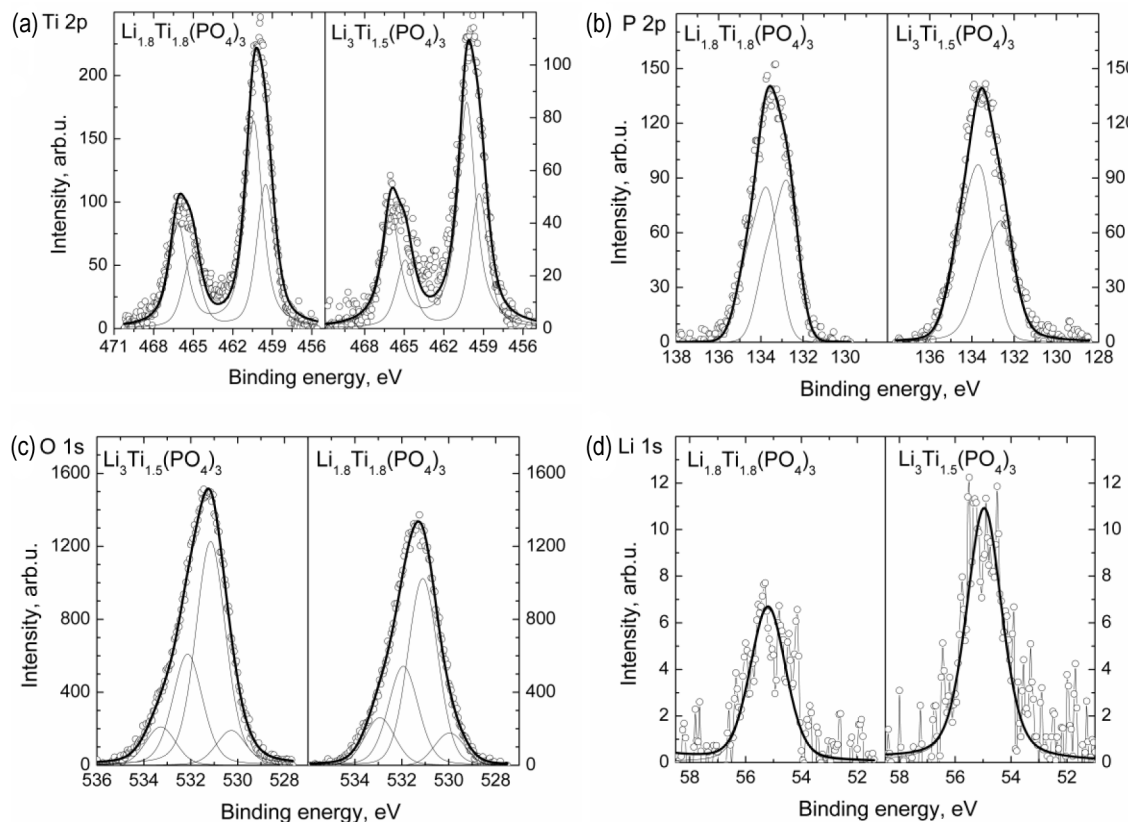


Fig. 4. Ti 2p (a), P 2p (b), O 1s (c), and Li 1s (d) core levels XP spectra of  $\text{Li}_{1+4x}\text{Ti}_{2-x}(\text{PO}_4)_3$  (where  $x = 0.2, 0.5$ ) compounds at room temperature.

[9, 13]. The relative amounts of elements with different binding energies, spin-orbit doublets' splitting energies of Ti 2p<sub>3/2</sub> core level XP spectra for investigated ceramics are presented in Table 2. The spin-orbit doublets assembled two peaks at different binding energy. The lower energy peaks of Ti 2p<sub>3/2</sub> spectra depend on stoichiometric parameters  $x$  of the investigated compounds and are in the range from 459.4 to 459.5 eV. The higher binding energy peaks are at 460.4 eV and do not depend on parameter  $x$ . The 2p<sub>3/2</sub> peaks at a lower binding energy (see Table 2) can be associated with a lower oxidation state (Ti<sup>3+</sup>). The peaks at a higher 2p<sub>3/2</sub> binding energy can be associated with the Ti<sup>4+</sup> valence state as in [14]. The results of the investigation of the Ti 2p core level XPS have shown that the increase of parameter  $x$  is associated with the increase of Ti<sup>4+</sup> amount. So, a ratio Ti<sup>4+</sup>/Ti<sup>3+</sup> changes from 1.5 for a compound with  $x = 0.2$  to 1.9 for a compound with  $x = 0.5$ . The binding energy splitting between lower and higher binding energy peaks is 5.6 and 5.7 eV, respectively. The authors of [13] reported that the binding energy splitting between Ti 2p<sub>3/2</sub> and Ti 2p<sub>1/2</sub> core level XPS was 5.4 eV. The P 2p core level XP spectra of Li<sub>1+4x</sub>Ti<sub>2-x</sub>(PO<sub>4</sub>)<sub>3</sub> (where  $x = 0.2, 0.5$ ) ceramics deconvoluted into two peaks as shown in Fig. 4(b). The peaks at the binding energy of 132.7 eV ( $x = 0.2, 50.4$  at. %), 132.5 eV ( $x = 0.5, 43.4$  at. %), and 133.6 eV ( $x = 0.2, 49.6$  at. %;  $x = 0.5, 56.6$  at. %) (see Table 2) can be associated with dominated groups (PO<sub>4</sub>)<sup>3-</sup> and (PO<sub>3</sub>)<sup>1-</sup> as in [15]. This difference in binding energies comes from different bonds of phosphorus such as P–O–P (or double bond P=O) and P–O–Ti (or Li). The splitting energy of P 2p spectra is 1.0 eV and does not depend on parameter  $x$ .

Figure 4(c) shows the characteristic fitting patterns of O 1s core level XP spectra of Li<sub>1+4x</sub>Ti<sub>2-x</sub>(PO<sub>4</sub>)<sub>3</sub> (where  $x = 0.2, 0.5$ ) ceramic surfaces. In the investigated compounds the O 1s spectrum has been deconvoluted into four peaks. The O 1s peak (see Table 2) at the binding energy of 531.1 eV (amount 55.1 at. % for  $x = 0.2$ ) and the peak at the binding energy of 531.0 eV for compounds with parameters  $x = 0.5$  can be attributed to the lattice oxygen and associated with groups (PO<sub>4</sub>)<sup>3-</sup> and (PO<sub>3</sub>)<sup>1-</sup> in the compounds. A small amount of O 1s peaks at the binding energy of 530.0 and 530.3 eV (8.2–8.5 at. %) can be attributed to oxygen forming relationships with the metal atoms, while other two O 1s

Table 2. Binding and splitting energies of Ti 2p, P 2p, O 1s, Li 1s core levels, amounts of peaks with certain binding energies and chi-square values in Li<sub>1+4x</sub>Ti<sub>2-x</sub>(PO<sub>4</sub>)<sub>3</sub> (where  $x = 0.2, 0.5$ ) compounds.

Core level	Binding energy $E$ , eV	Splitting $\Delta E$ , eV	Amount, at. %	$\chi^2$
Li <sub>1.8</sub> Ti <sub>1.8</sub> (PO <sub>4</sub> ) <sub>3</sub>				
Ti 2p <sub>3/2</sub>	459.5	5.6	39.1	0.6
	460.4	5.7	60.9	
P 2p <sub>3/2</sub>	132.7	1.0	50.4	0.8
	133.6	1.0	49.6	
O 1s	530.3		8.5	0.9
	531.2		55.1	
	532.1		27.4	
	533.3		8.0	
Li 1s	55.3		100	0.1
Li <sub>3</sub> Ti <sub>1.5</sub> (PO <sub>4</sub> ) <sub>3</sub>				
Ti 2p <sub>3/2</sub>	459.4	5.6	34.7	0.5
	460.4	5.7	65.3	
P 2p <sub>3/2</sub>	132.5	1.0	43.4	0.7
	133.6	1.0	56.6	
O 1s	530.0		8.2	1.2
	531.1		50.6	
	532.0		28.1	
	533.2		13.1	
Li 1s	55.0		100	0.2

peaks can be assigned to the oxygen in hydroxyl environment (OH) or CO as in ceramics [9, 16]. On the other hand, LiTiPO<sub>5</sub>, Li<sub>4</sub>(P<sub>2</sub>O<sub>7</sub>) exist in the investigated compounds as impurities, and these can influence the binding energies and amount of peaks.

The Li 1s signal is of very low intensity but in all investigated compounds only a single peak with the amount of 100 at. % was found (Table 2). These results can be assigned to the fact that in the lattice of the compounds one energy position for Li ions dominates. The binding energy of Li 1s core level XPS changed in the range from 55.3 to 55.0 eV and these results accord with [17]. A decrease of parameter  $x$  determines an increase of the binding energy of Li 1s core level XPS. It is reported in [18] that for the Li<sub>0.8</sub>CoO<sub>4</sub> composition the Li 1s single peak has been observed at 55.4 eV and their binding energy and the number of peaks depend on Li amount in the compound. The authors concluded that Li ions occupy two different positions. The results of the NMR study of LiTi<sub>2-x</sub>Zr<sub>x</sub>(PO<sub>4</sub>)<sub>3</sub> composition have shown that Li ions occupy two different positions

in the lattice [4]. The results of NMR investigations of the NASICON-type framework structure  $\text{Li}_{1.3}\text{Al}_{0.15}\text{Y}_{0.15}\text{Ti}_{1.7}(\text{PO}_4)_3$  compound showed only one Li ion position in the lattice [7].

The characteristic frequency dependences of the real part of complex conductivity ( $\sigma'$ ) of  $\text{Li}_{1+4x}\text{Ti}_{2-x}(\text{PO}_4)_3$  (where  $x = 0.2, 0.5$ ) ceramics measured at the temperature  $T = 300$  K are shown in Fig. 5. In

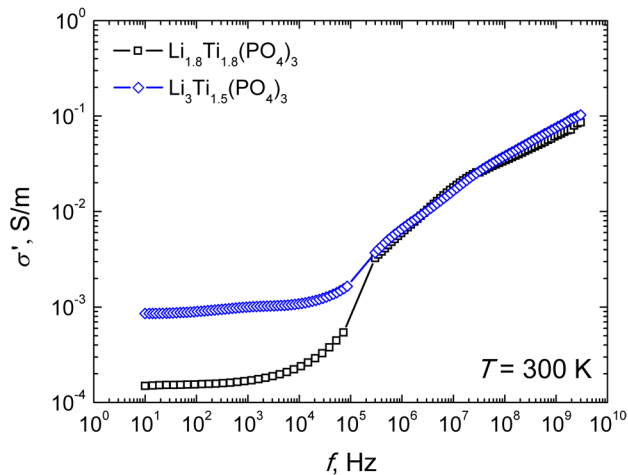


Fig. 5. Frequency dependences of total conductivities of  $\text{Li}_{1+4x}\text{Ti}_{2-x}(\text{PO}_4)_3$  (where  $x = 0.2, 0.5$ ) measured at  $T = 300$  K temperature.

the frequency range from 10 Hz to 100 kHz the ceramics were investigated by the four-probe method, and in the microwave range the measurements were carried out by the coaxial technique. Two dispersion regions in  $\sigma'$  spectra for all investigated compounds were found. The low frequency dispersion range of  $\sigma'$  is caused by ion transport in grain boundary because high frequency range is attributed to ion transport in grain as in [19–22]. The processes are thermally activated and dispersion regions shift towards higher frequencies as temperature increases. This phenomenon is typical of relaxation-type dispersions. In Fig. 6 the characteristic frequency dependences of the real part of complex conductivity ( $\sigma'$ ) of  $\text{Li}_3\text{Ti}_{1.5}(\text{PO}_4)_3$  ceramics measured at different temperatures are shown. The total conductivities ( $\sigma_{\text{tot}}$ ) of the ceramics were derived from temperature dependences of the plateau of  $\sigma'$  ( $f$ ) dependences and complex specific resistance  $\rho''(\sigma')$  plots (see Fig. 7). The temperature dependences of bulk ionic conductivities  $\sigma_b$  have been found from complex plane plots

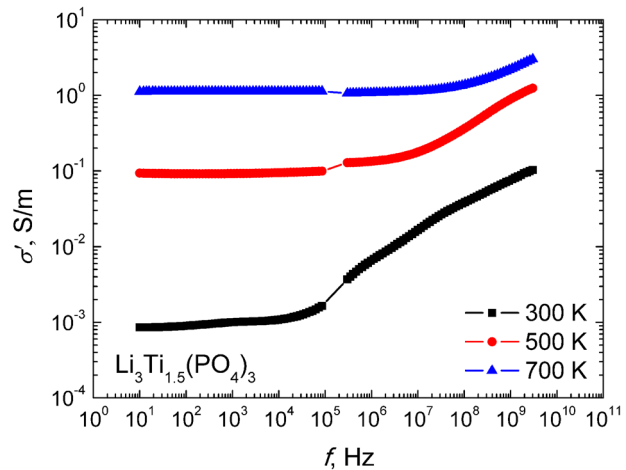


Fig. 6. Characteristic frequency dependences of the real part of complex conductivity of  $\text{Li}_3\text{Ti}_{1.5}(\text{PO}_4)_3$  ceramics measured at different temperatures.

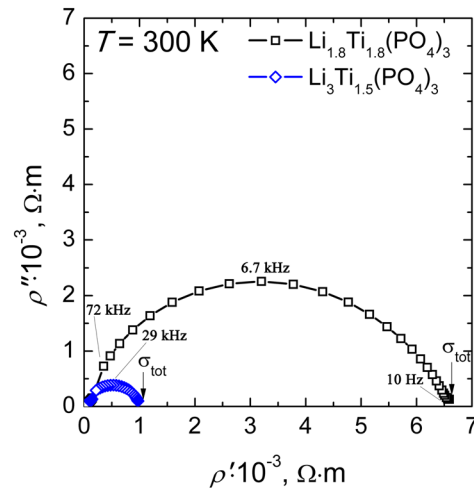


Fig. 7. Complex specific electrical resistivity plots of  $\text{Li}_{1+4x}\text{Ti}_{2-x}(\text{PO}_4)_3$  (where  $x = 0.2, 0.5$ ) ceramics at temperature  $T = 300$  K.

of conductivity at different temperatures as shown in Fig. 8. The temperature dependences of  $\sigma_{\text{tot}}$  and  $\sigma_b$  of  $\text{Li}_{1+4x}\text{Ti}_{2-x}(\text{PO}_4)_3$  (where  $x = 0.2, 0.5$ ) ceramic samples are shown in Fig. 9. The maximal value of  $\sigma_{\text{tot}}$  was found for a compound with parameter  $x = 0.5$ . The increase of the parameter  $x$  leads to the increase of the value of  $\sigma_b$ . The activation energies of  $\sigma_{\text{tot}}$  and  $\sigma_b$  were found from the slopes of the Arrhenius plots. From the maxima of  $\rho''(f)$  at different temperatures, the characteristic relaxation frequency  $f_b$  in the grain was determined as in [23, 24]. In Fig. 10 the characteristic frequency dependences of  $\rho''$  at the temperature of 300 K of  $\text{Li}_{1+4x}\text{Ti}_{2-x}(\text{PO}_4)_3$  (where  $x = 0.2, 0.5$ ) compounds

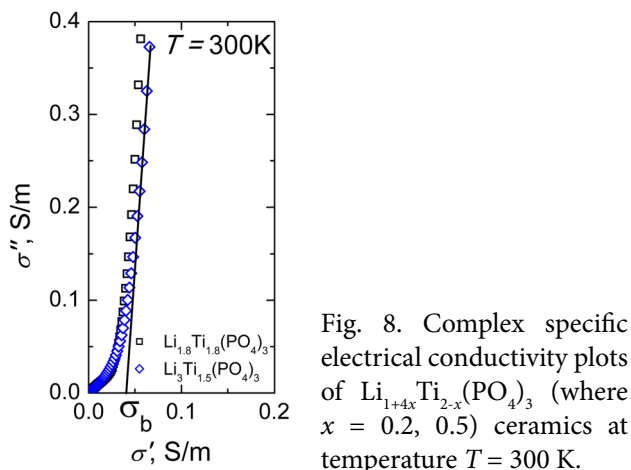


Fig. 8. Complex specific electrical conductivity plots of  $\text{Li}_{1+4x}\text{Ti}_{2-x}(\text{PO}_4)_3$  (where  $x = 0.2, 0.5$ ) ceramics at temperature  $T = 300$  K.

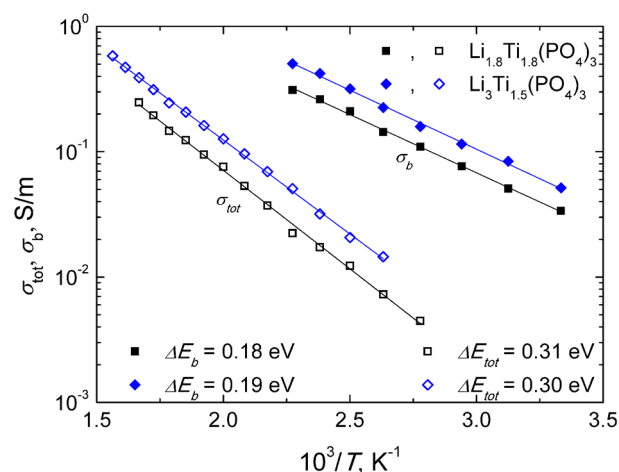


Fig. 9. Arrhenius plots of total and bulk conductivities of  $\text{Li}_{1+4x}\text{Ti}_{2-x}(\text{PO}_4)_3$  (where  $x = 0.2, 0.5$ ) ceramics.

are shown. The relaxation frequency is thermally activated and increases with temperature according to the Arrhenius law:  $f_b = f_0 \exp(-\Delta E_f/kT)$ , where  $f_0$  is an attempt frequency related to the lattice vibrations,  $\Delta E_f$  is the activation energy of  $f_b$ ,  $k$  is the Boltzmann constant. The activation energies  $\Delta E_f$  were calculated from the slopes of the Arrhenius plots of  $f_b$ . Figure 11 shows the temperature dependences of  $f_b$ . Table 3 summarizes our experimental results of the investigation of  $\sigma_{\text{tot}}$ ,  $\sigma_b$ , their activation energies, and  $f_b$  and activation energy of characteristic relaxation frequency  $\Delta E_f$ . The values of the activation energy of ionic conductivity in grains  $\Delta E_b$  and the activation energy of characteristic relaxation frequency  $\Delta E_f$  are similar. The activation energy  $\Delta E_f$  associates with the activation energy of mobility of charge carriers in grains. As we found that the values of activation energies of the bulk ionic conductivities of investi-

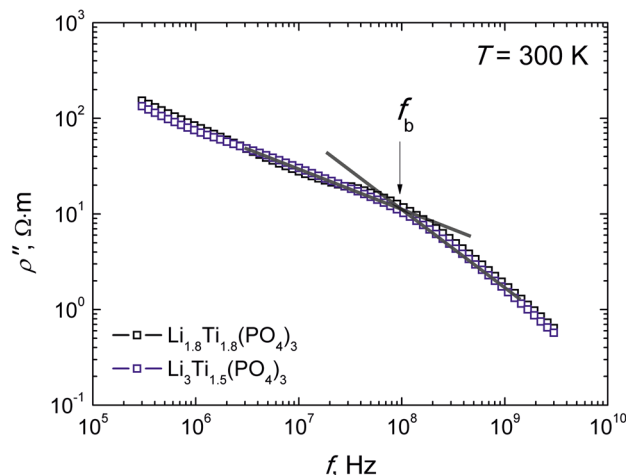


Fig. 10. Frequency dependences of the imaginary part of complex resistivity of  $\text{Li}_{1+4x}\text{Ti}_{2-x}(\text{PO}_4)_3$  (where  $x = 0.2, 0.5$ ) ceramics at the temperature  $T = 300$  K.

gated ceramics are similar to the activation energies of relaxation frequency, which can be attributed to mobility of  $\text{Li}^+$  ions, the concentration of charge carriers remains constant with changing temperature. The temperature dependences of the dielectric permittivity  $\epsilon'$  were investigated at the frequency of 1 GHz. The values of  $\epsilon'$  at the temperature of 300 K of  $\text{Li}_{1+4x}\text{Ti}_{2-x}(\text{PO}_4)_3$  ceramics where  $x = 0.2$  and  $0.5$  were found to be 9.69 and 10.82, respectively. These  $\epsilon'$  values at room temperature are characteristic of NASICON-type compounds [19, 25]. For example, the values of dielectric permittivity of  $\text{Li}^+$  conducting NASICON-type compounds  $\text{Li}_{1+x}\text{Y}_y\text{Ti}_{2-y}(\text{PO}_4)_3$

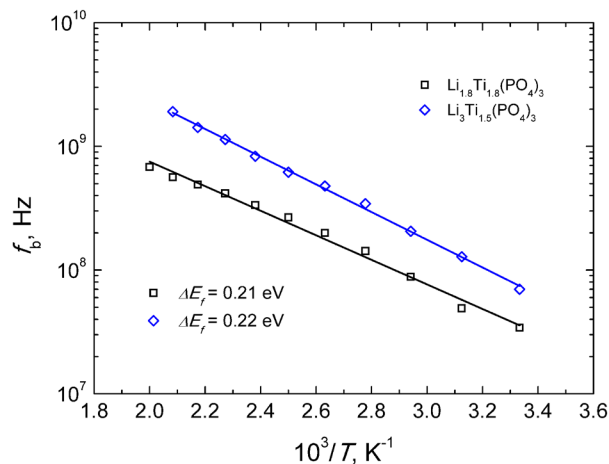


Fig. 11. Temperature dependences of relaxation frequency in the bulk of  $\text{Li}_{1+4x}\text{Ti}_{2-x}(\text{PO}_4)_3$  (where  $x = 0.2, 0.5$ ) ceramics.

Table 3.  $\sigma_b$  ( $T = 300$  K),  $\sigma_{tot}$  ( $T = 380$  K),  $f_b$  ( $T = 300$  K) and their activation energies of  $\text{Li}_{1+4x}\text{Ti}_{2-x}(\text{PO}_4)_3$  (where  $x = 0.2, 0.5$ ) samples.

Compound	$\sigma_b$ , S/m	$\Delta E_{\sigma b}$ , eV	$\sigma_{tot}$ , S/m	$\Delta E_{\sigma_{tot}}$ , eV	$f_b$ , MHz	$\Delta E_p$ , eV	$\epsilon'$
	$T = 300$ K		$T = 380$ K		$T = 300$ K		$T = 300$ K
$\text{Li}_{1.8}\text{Ti}_{1.8}(\text{PO}_4)_3$	0.0338	0.18	0.0073	0.31	34	0.21	9.69
$\text{Li}_3\text{Ti}_{1.5}(\text{PO}_4)_3$	0.0515	0.19	0.0146	0.30	70	0.22	10.82

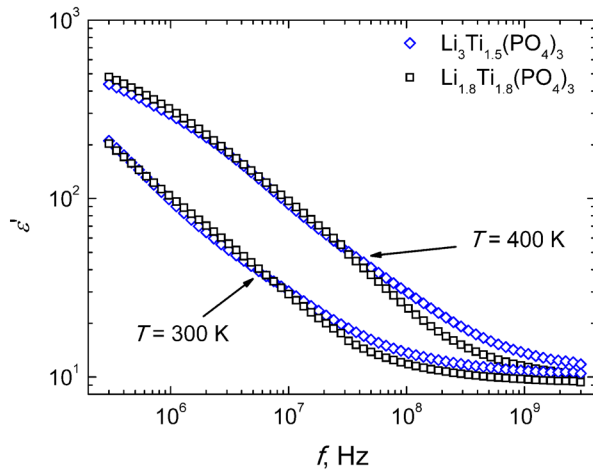


Fig. 12. Frequency dependences of  $\epsilon'$  ( $f$ ) for  $\text{Li}_{1+4x}\text{Ti}_{2-x}(\text{PO}_4)_3$  (where  $x = 0.2, 0.5$ ) ceramics at the temperatures of 300 and 400 K.

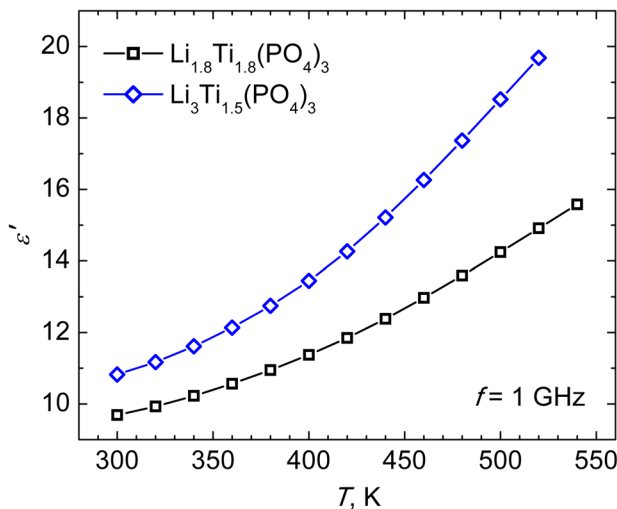


Fig. 13. Temperature dependences of the real part of complex dielectric permittivity measured at 1 GHz frequency.

(where  $x, y = 0.3, 0.4$ ) were found to be  $\epsilon' = 10$  and increase with temperature [19]. This frequency at the temperature  $T = 400$  K is higher than Maxwell relaxation frequency  $f_M = \sigma_b / 2\pi\epsilon'\epsilon_0$  (where  $\epsilon_0 = 8.85 \cdot 10^{-12}$  F/m is the dielectric constant of

the vacuum). The frequency dependences of  $\epsilon'$  for  $\text{Li}_{1+4x}\text{Ti}_{2-x}(\text{PO}_4)_3$  (where  $x = 0.2, 0.5$ ) ceramics at the temperatures of 300 and 400 K are shown in Fig. 12. The results of the measurements of dependences  $\epsilon'(f)$  showed that the frequency of 1 GHz is higher than the frequency dispersion regions for both compounds. The calculated Maxwell relaxation frequency at temperature  $T = 400$  K for compounds with  $x = 0.2$  and  $0.5$  were found to be 332 and 426 MHz, respectively. The temperature dependences of  $\epsilon'$  of  $\text{Li}_{1+4x}\text{Ti}_{2-x}(\text{PO}_4)_3$  (where  $x = 0.2, 0.5$ ) ceramics are shown in Fig. 13. The values  $\epsilon'$  at the temperature of 300 K of  $\text{Li}_{1+4x}\text{Ti}_{2-x}(\text{PO}_4)_3$  (where  $x = 0.2, 0.5$ ) ceramics are summarized in Table 3 too. The increase of the values of  $\epsilon'$  with temperature of the investigated compounds can be caused by contribution of the migration polarization of lithium ions, vibration of the lattice, and electronic polarization.

#### 4. Conclusions

The results of the XRD investigations from the powder showed that  $\text{Li}_{1+4x}\text{Ti}_{2-x}(\text{PO}_4)_3$  (where  $x = 0.2, 0.5$ ) compounds belong to the rhombohedral symmetry (space group  $R\bar{3}c$ ). The Ti 2p core level XPS peaks at the binding energy in the range of 459.4 to 459.5 eV were associated with  $\text{Ti}^{3+}$  oxidation states, and the peaks at the binding energy of 460.4 eV can be associated with the  $\text{Ti}^{4+}$  valence state. In all the investigated compounds the O 1s spectrum has been deconvoluted into four peaks. It was ascertained that there are four different kinds of oxygen on the ceramics surface, including lattice oxygen, oxygen in the OH and CO groups. The deconvolution into two peaks of P 2p XP spectra in the investigated ceramics showed different amounts of  $\text{P}^{5+}$  and  $\text{P}^{3+}$  valence states. The splitting energy between P 2p<sub>3/2</sub> and P 2p<sub>1/2</sub> spectra is 1.0 eV and does not depend on parameter  $x$ . Only single peaks with the amount of 100 at. % in Li 1s core level XP spectra were found. Two relaxation dispersion regions of electrical properties are attributed to Li ion migration in grain

boundary and bulk of the investigated ceramics. The activation energy of characteristic relaxation frequency correlates with the activation energy of bulk conductivity of the investigated compounds. The temperature dependence of bulk conductivity is related to the Li<sup>+</sup> ion mobility, which increases as temperature increases.

### Acknowledgements

This work was supported by projects No. TAP LLT 03/2012 and No. TAP LZ 06/2012 of the Research Council of Lithuania and by the Latvian state budget according to the National Research Program in Material sciences (IMIS). Tomas Šalkus also wishes to acknowledge the Research Council of Lithuania for funding this work according to the project “Postdoctoral Fellowship Implementation in Lithuania”.

### References

- [1] G. Adachi, N. Imanaka, E. Sugimoto, Y. Sadaoka, N. Yasuda, T. Har, and M. Nagata, United States Patent No. 4,985,317, Jan. 15, 1991.
- [2] P. Birke, F. Salam, S. Doring, and W. Weppner, A first approach to a monolithic all solid state inorganic lithium battery, *Solid State Ionics* **118**, 149–157 (1999), [http://dx.doi.org/10.1016/S0167-2738\(98\)00462-7](http://dx.doi.org/10.1016/S0167-2738(98)00462-7)
- [3] H. Aono, E. Sugimoto, Y. Sadaoka, N. Imanaka, and G.-Y. Adachi, Ionic conductivity of solid electrolytes based on lithium titanium phosphate, *J. Electrochem. Soc.* **137**, 1023–1027 (1990), <http://dx.doi:10.1149/1.2086597>
- [4] M.A. Subramanian, R. Subramanian, and A. Clearfield, Lithium ion conductors in the system AB(IV)<sub>2</sub>(PO<sub>4</sub>)<sub>3</sub> (B = Ti, Zr and Hf), *Solid State Ionics* **18–19**(1), 562–569 (1986), [http://dx.doi.org/10.1016/0167-2738\(86\)90179-7](http://dx.doi.org/10.1016/0167-2738(86)90179-7)
- [5] K. Arbi, J.M. Rojo, and J. Sanz, Lithium mobility in titanium based Nasicon Li<sub>1+x</sub>Ti<sub>2-x</sub>Al<sub>x</sub>(PO<sub>4</sub>)<sub>3</sub> and LiTi<sub>2-x</sub>Zr<sub>x</sub>(PO<sub>4</sub>)<sub>3</sub> materials followed by NMR and impedance spectroscopy, *J. Eur. Ceram. Soc.* **27**, 4215–4218 (2007), <http://dx.doi.org/10.1016/j.jeurceramsoc.2007.02.118>
- [6] K. Arbi, M.G. Lazarraga, D. Ben Hassen Chehimi, M. Ayadi-Trabelsi, J.M. Rojo, and J. Sanz, Lithium mobility in Li<sub>1.2</sub>Ti<sub>1.8</sub>R<sub>0.2</sub>(PO<sub>4</sub>)<sub>3</sub> compounds (R = Al, Ga, Sc, In) as followed by NMR and impedance spectroscopy, *Chem. Mater.* **16**, 255–262 (2004), <http://pubs.acs.org/doi/full/10.1021/cm030422i>
- [7] T. Šalkus, E. Kazakevičius, A. Kežionis, A. Dindune, A. Kanepe, J. Ronis, J. Emery, A. Boulant, O. Bohne, and A.F. Orliukas, Peculiarities of ionic transport in Li<sub>1.3</sub>Al<sub>0.15</sub>Y<sub>0.15</sub>Ti<sub>1.7</sub>(PO<sub>4</sub>)<sub>3</sub> ceramics, *J. Phys.: Condens. Matter* **21**(18), 185502 (2009), <http://iopscience.iop.org/0953-8984/21/18/185502/>
- [8] W. Paszkowicz, INDEXING – program for indexing powder patterns of cubic, tetragonal, hexagonal and orthorhombic substances on personal computers, *J. Appl. Crystallogr.* **22**, 186–187 (1989), <http://dx.doi.org/10.1107/S0021889889099802>
- [9] A.F. Orliukas, T. Šalkus, A. Kežionis, A. Dindune, Z. Kanepe, J. Ronis, V. Venckutė, V. Kazlauskienė, J. Miškinis, and A. Lukauskas, Structure and broadband impedance spectroscopy of Li<sub>1.3</sub>Al<sub>y</sub>Y<sub>x-y</sub>Ti<sub>1.7</sub>(PO<sub>4</sub>)<sub>3</sub> (x = 0.3; y = 0.1, 0.2) solid electrolyte ceramics, *Solid State Ionics* **225**, 620–625 (2012), <http://dx.doi.org/10.1016/j.ssi.2012.05.011>
- [10] A. Kežionis, P. Butvilas, T. Šalkus, S. Kazlauskas, D. Petrulionis, T. Žukauskas, E. Kazakevičius, and A.F. Orliukas, Four-electrode impedance spectrometer for investigation of solid ion conductors, *Rev. Sci. Instrum.* **84**, 013902 (2013), <http://dx.doi.org/10.1063/1.4774391>
- [11] A. Kežionis, E. Kazakevičius, T. Šalkus, and A. Orliukas, Broadband high frequency impedance spectrometer with working temperatures up to 1200 K, *Solid State Ionics* **188**, 110–113 (2011), <http://dx.doi.org/10.1016/j.ssi.2010.09.034>
- [12] R. D. Shannon, Revised effective ionic radii and systematic studies of interatomic distances in halides and chalcogenides, *Acta Crystallogr.* **A32**, 751–767 (1976), <http://dx.doi.org/10.1107/S0567739476001551>
- [13] Q.-H. Wu, J.-M. Xu, Q.-C. Zhuang, and S.-G. Sun, X-ray photoelectron spectroscopy of LiM<sub>0.05</sub>Mn<sub>1.95</sub>O<sub>4</sub> (M = Ni, Fe and Ti), *Solid State Ionics* **177**, 1483–1488 (2006), <http://dx.doi.org/10.1016/j.ssi.2006.06.020>
- [14] B.V.R. Chowdari, G.V. Subba Rao, and G.Y.H. Lee, XPS and ionic conductivity studies on Li<sub>2</sub>O–Al<sub>2</sub>O<sub>3</sub>–(TiO<sub>2</sub> or GeO<sub>2</sub>)–P<sub>2</sub>O<sub>5</sub> glass–ceramics, *Solid State Ionics* **136–137**, 1067–1075 (2000), [http://dx.doi.org/10.1016/S0167-2738\(00\)00500-2](http://dx.doi.org/10.1016/S0167-2738(00)00500-2)
- [15] J.-Y. Luo, L.-J. Chen, Y.-J. Zhao, P. He, and Y.-Y. Xia, The effect of oxygen vacancies on the structure and electrochemistry of LiTi<sub>2</sub>(PO<sub>4</sub>)<sub>3</sub> for lithium-ion batteries: A combined experimental and theoretical study, *J. Power Sources* **194**, 1075–1080 (2009), <http://dx.doi.org/10.1016/j.jpowsour.2009.06.050>
- [16] Q. Xu, D.P. Huang, W. Chen, H. Wang, B.-T. Wang, and R.-Z. Yuan, X-ray photoelectron spectroscopy investigation on chemical states of oxygen on surfaces of mixed electronic–ionic conducting La<sub>0.6</sub>Sr<sub>0.4</sub>Co<sub>1-y</sub>Fe<sub>y</sub>O<sub>3</sub> ceramics, *Appl. Sur. Sci.* **228**, 110–114 (2004), <http://dx.doi.org/10.1016/j.apsusc.2003.12.030>
- [17] T. Šalkus, A. Kežionis, V. Kazlauskienė, J. Miškinis, A. Dindune, Z. Kanepe, J. Ronis, and A.F. Orliukas, Surface and impedance spectroscopy studies of

- $\text{Li}_{2.8}\text{Sc}_{1.8-y}\text{Y}_y\text{Zr}_{0.2}(\text{PO}_4)_3$  (where  $y = 0, 0.1$ ) solid electrolyte ceramics, *Mater. Sci. Eng.* **B 172**, 156–162 (2010), <http://dx.doi.org/10.1016/j.mseb.2010.05.002>
- [18] M.S. Bhuvaneswari, S. Selvasekarapandian, S. Fujihara, and S. Koji, Structural, XPS and impedance analysis of  $\text{Li}_x\text{CoVO}_4$  ( $x = 0.8, 1.0, 1.2$ ), *Solid State Ionics* **177**, 121–127 (2006), <http://dx.doi.org/10.1016/j.ssi.2005.09.011>
- [19] R. Sobiestianskas, A. Dindune, Z. Kanepe, J. Ronis, A. Kežionis, E. Kazakevičius, and A. Orliukas, Electrical properties of  $\text{Li}_{1+x}\text{Y}_y\text{Ti}_{2-y}(\text{PO}_4)_3$  (where  $x, y=0.3; 0.4$ ) ceramics at high frequencies, *Mater. Sci. Eng., B* **76**, 184–192 (2000), [http://dx.doi.org/10.1016/S0921-5107\(00\)00437-2](http://dx.doi.org/10.1016/S0921-5107(00)00437-2)
- [20] W. Bogusz, J.R. Dygas, F. Krok, A. Kežionis, R. Sobiestianskas, E. Kazakevičius, and A. Orliukas, Electrical conductivity dispersion in Co-doped NASICON samples, *Phys. Stat. Sol. (a)* **183**, 323–330 (2001), [http://dx.doi.org/10.1002/1521-396X\(200102\)183:2<323::AID-PSSA323>3.0.CO;2-6](http://dx.doi.org/10.1002/1521-396X(200102)183:2<323::AID-PSSA323>3.0.CO;2-6)
- [21] M. Cretin and P. Fabry, Comparative study of lithium ion conductors in the system  $\text{Li}_{1+x}\text{Al}_x\text{A}_{2-x}^{\text{IV}}(\text{PO}_4)_3$  with  $\text{A}^{\text{IV}}=\text{Ti}$  or  $\text{Ge}$  and  $0 \leq x \leq 0.7$  for use as  $\text{Li}^+$  sensitive membranes, *J. Eur. Ceram. Soc.* **19**, 2931–2940 (1999), [http://dx.doi.org/10.1016/S0955-2219\(99\)00055-2](http://dx.doi.org/10.1016/S0955-2219(99)00055-2)
- [22] M. Godickemeier, B. Michel, A. Orliukas, P. Bohac, K. Sasaki, L. Gauckler, H. Heinrich, P. Schwander, G. Kostorz, H. Hofmann, and O. Frei, Effect of intergranular glass films on the electrical conductivity of 3Y-TZP, *J. Mater. Res.* **9**(5), 1228–1240 (1994), <http://dx.doi.org/10.1557/JMR.1994.1228>
- [23] T. Šalkus, A. Dindune, Z. Kanepe, J. Ronis, A. Určinskas, A. Kežionis, and A.F. Orliukas, Lithium ion conductors in the system  $\text{Li}_{1+y}\text{Ge}_{2-x-y}\text{Ti}_x\text{Al}_y(\text{PO}_4)_3$  ( $x = 0.1 \div 0.3, y = 0.07 \div 0.21$ ), *Solid State Ionics* **178**, 1282–1287 (2007), <http://dx.doi.org/10.1016/j.ssi.2007.07.002>
- [24] A.F. Orliukas, T. Šalkus, A. Dindune, Z. Kanepe, J. Ronis, A. Určinskas, E. Kazakevičius, A. Kežionis, V. Kazlauskienė, and J. Miškinis, Synthesis, structure and electrical properties of  $\text{Li}_{1+x+y}\text{Sc}_x\text{Y}_y\text{Ti}_{2-x-y}(\text{PO}_4)_3$  ( $x = 0.15-0.3, y = 0.01-0.15$ ) ceramics, *Solid State Ionics* **179**, 159–163 (2008), <http://dx.doi.org/10.1016/j.ssi.2007.12.036>
- [25] A.F. Orliukas, A. Dindune, Z. Kanepe, J. Ronis, B. Bogdonas, and A. Kežionis, Synthesis and peculiarities of electric properties of  $\text{Li}_{1.3}\text{Zr}_{1.4}\text{Ti}_{0.3}\text{Al}_{0.3}(\text{PO}_4)_3$  solid electrolyte ceramics, *Electrochim. Acta* **51**, 6194–6198 (2006), <http://dx.doi.org/10.1016/j.electacta.2005.11.049>

## Li<sub>1+4x</sub>Ti<sub>2-x</sub>(PO<sub>4</sub>)<sub>3</sub> KIETŪJŲ KERAMINIŲ ELEKTROLITŲ RENTGENO SPINDULIŲ FOTOELEKTRONINĖ IR BENDROSIOS VARŽOS PLAČIAJUOSTĖ SPEKTROSKOPIJA

A. F. Orliukas<sup>a</sup>, V. Venckutė<sup>a\*</sup>, J. Miškinis<sup>b</sup>, V. Kazlauskienė<sup>b</sup>, D. Petrulionis<sup>a</sup>, T. Šalkus<sup>a</sup>,  
A. Dindune<sup>c</sup>, Z. Kanepe<sup>c</sup>, J. Ronis<sup>c</sup>, T. Žukauskas<sup>a</sup>, A. Maneikis<sup>d</sup>, A. Kežionis<sup>a</sup>

<sup>a</sup> *Vilniaus universiteto Fizikos fakultetas, Vilnius, Lietuva*

<sup>b</sup> *Vilniaus universiteto Taikomųjų mokslų institutas, Vilnius, Lietuva*

<sup>c</sup> *Rygos technikos universiteto Neorganinės chemijos institutas, Salaspilis, Latvija*

<sup>d</sup> *Fizinių ir technologijos mokslų centro Puslaidininkių fizikos institutas, Vilnius, Lietuva*

### Santrauka

Li<sub>1+4x</sub>Ti<sub>2-x</sub>(PO<sub>4</sub>)<sub>3</sub> ( $x = 0,2; 0,5$ ) kietųjų elektrolitų milteliai buvo sintezuoti kietųjų kūnų reakcijos metodu. Kristalinė junginių struktūra tirta rentgeno spindulių difrakcijos metodu. Tyrimams naudotas Bruker D8 difraktometras bei CuK<sub>α1</sub> spinduliuotė. Kristalinių gardelių parametrų skaičiavimams naudotos TOPAS v.4.1 ir SCANIX v.2.16 (Matpol) programos. Kambario temperatūroje minėtieji junginiai priklauso NASICON kristalinio tipo romboedrinei simetrijai (erdvinė simetrijos grupė  $R\bar{3}c$ ). Jų elementariausias kristalines gardses sudaro šeši formuliniai vienetai. Abiejuose junginiuose aptinkamos LiTiPO<sub>5</sub> ir Li<sub>4</sub>(P<sub>2</sub>O<sub>7</sub>) kristalinės priemaišos, kurių struktūros atitinkamai priklauso ortorombinei ir triklinei simetrijoms.

Skenuojančio elektroninio mikroskopo (SEM), rentgeno spindulių energijos dispersijos (EDS), Rentgeno spindulių fotoelektronų bei pilnutinės varžos spektrometriniams tyrimams naudoti keraminiai bandiniai. Li<sub>1,8</sub>Ti<sub>1,8</sub>(PO<sub>4</sub>)<sub>3</sub> ir Li<sub>3</sub>Ti<sub>1,5</sub>(PO<sub>4</sub>)<sub>3</sub> keramikos buvo kepamos po 1 h atitinkamai 1363 K ir 923 K temperatūrose. Keramikų santykiniai tankiai siekia 81–95 % jų teorinio tankio.

SEM/EDS tyrimams naudotas TM 3000 – Hitachi analizatorius. SEM tyrimai parodė, kad keramikų paviršių mikrostruktūros yra panašios ir jų dominuojantys kristalinių dydžiai kinta 4–10 μm ribose. ED spektruose be pagrindinių elementų aptinkamos Al (0,457–0,585 sv. %) bei Si (0,220–0,201 sv. %) priemaišos, kurios kepinant keramiką galėjo patekti nuo padėklų.

Rentgeno spindulių fotoelektronų spektrų tyrimams naudota Al K<sub>α</sub> ( $h\nu = 1486,6$  eV) spinduliuotė, o spektrų analizei taikyta XPSPEAK 41 programa. Gauti Ti 2p, P 2p, O 1s ir Li 1s rentgeno fotoelektronų spektrai. Ti 2p spektrų analizė rodo, kad Ti šiuose junginiuose

gali būti trivalentis ir keturvalentis. Ti<sup>3+</sup> ir Ti<sup>4+</sup> kiekis priklauso nuo junginių stochiometrijos veiksnio  $x$ . P 2p spektrą sudaro du sandai. Tai gali būti siejama su skirtingais fosforo formuojamais cheminiais ryšiais, kurie apsprendžia susidarantią struktūrą su vyraujančiomis (PO<sub>4</sub>)<sup>3-</sup> ar (PO<sub>3</sub>)<sup>1-</sup> grupėmis. Skirtingas P 2p<sub>3/2</sub> smailių ryšių energijas gali sąlygoti skirtingi P–O–P, P=O bei P–O–Ti ryšiai. P 2p<sub>3/2</sub> ir P 2p<sub>1/2</sub> plėtinių energija nepriklauso nuo  $x$  ir yra lygi 1 eV. O 1s spektrus sudaro keturios smailės su skirtingomis ryšio energijomis. Tai gali būti siejama su gardeliniais deguonimi, sudarančiu grupes su fosforu (PO<sub>4</sub>)<sup>3-</sup> arba (PO<sub>3</sub>)<sup>1-</sup> (artima 531 eV), nedideliu kiekiu deguonies formuojančiu ryšius tik su metalo atomais (530 eV) bei bandinio paviršiuje susidariusiais dariniais su (OH) bei (CO). Junginių Li 1s spektre stebima viena smailė ties ryšio energija 55,3 eV ( $x = 0,2$ ) bei 55,0 eV ( $x = 0,5$ ). Tai nusako vieną Li energinę padėtį tirtų junginių gardelėse.

Elektrinės keramikų savybės tirtos 10 Hz – 3 GHz dažnių ir 300–700 K temperatūrų intervaluose. Žemųjų dažnių (iki 1 MHz) diapazone elektriniams keramikų tyrimams naudotas keturių elektrodų metodas, o mikrobangose jos tirtos taikant bendraašę tyrimų techniką. Keramikų elektrinio laidumo spektruose reiškiasi dvi relaksacinio tipo dispersijos, kurios siejamos su Li<sup>+</sup> jonų pernaša tarpkristalitinėse sandūrose bei kristalituose. Didėjant stochiometrijos veiksniai  $x$  keramikų kristalitinio laidumas didėja. Temperatūrinės keramikų tarpkristalitinio ir kristalitinio laidumų priklausomybės tenkina Arenijaus dėsnį. Didėjant  $x$  keramikų dielektrinė skvarba didėja. Keramikų dielektrinės skvarbos reikšmę sąlygoja jonų migracinės, jonų tampriosios bei elektroninės poliarizacijos indėliai.